Journal of Solid State Chemistry **161,** 327–331 (2001)
doi:10.1006/jssc.2001.9321, available online at http://www.idealibrary.com on IDEAL®

A New Silicon-Doped Cation-Deficient Thiospinel, $Cu_{5.52(8)}Si_{1.04(8)}\square_{1.44}Fe_4Sn_{12}S_{32}$: Crystal Structure, Mössbauer Studies, and Electrical Properties

G. Garg,* S. Bobev,† A. Roy,‡ J. Ghose,‡ D. Das,§ and A. K. Ganguli*,[1]

*Department of Chemistry, Indian Institute of Technology, New Delhi 110 016, India; †Department of Chemistry and Biochemistry, University of Notre Dame, South Bend, Indiana 46556; ‡Department of Chemistry, Indian Institute of Technology, Kharagpur 721 302, India; and §Inter-University Consortium for D.A.E. Facilities, Calcutta Centre, 3/LB-8, Salt Lake, Calcutta 700 091, India

Received April 23, 2001; in revised form July 11, 2001; accepted July 23, 2001

Starting from pure metals and sulfur in evacuated silica tubes, single crystals of $Cu_{5.52(8)}Si_{1.04(8)}\square_{1.44}Fe_4Sn_{12}S_{32}$ have been obtained by quenching from 680°C. The above cation-deficient thiospinel crystallizes in the $Fd\bar{3}m$ space group with $a = 10.3322(6)$ Å. Si doping leads to additional vacancies in the copper site. ^{119}Sn Mössbauer data show the presence of Sn in II as well as IV oxidation states and all the Sn is present in the octahedral 16*d* sites. ^{57}Fe Mössbauer studies show Fe to be present in the octahedral sites in both II and III oxidation states. The above thiospinel shows semiconducting behavior with resistivity of $\sim 1 \times 10^2$ Ω-cm at room temperature and a small band gap of ~ 0.1 eV.

Key Words: **Mössbauer spectroscopy; thiospinels; electrode material; crystal structure; electrical transport.**

INTRODUCTION

Lithium-intercalated spinel-related compounds (AB_2X_4) are considered as useful reversible cathode materials in an aprotic electrolyte battery system. The X anions in the spinels are arranged in a cubic close-packing (ccp) arrangement in 32e sites. The B cations occupy the 16*d* octahedral sites and A cations are present in the 8*a* tetrahedral sites defined by the anion array. In addition, there are other tetrahedral and octahedral sites, which are empty. In order to improve the diffusion of lithium ions, certain ions can be removed from the spinel structure. Copper extraction by treatment with mild oxidizing agents has been shown in $Cu_xMo_6S_8$ (1,2) and $CuZr_2S_4$ (3). These materials seem to have immense potential for applications as cathode materials (4). Apart from the above ternary thiospinels, several quaternary thiospinels of the type $Cu_2MSn_3S_8$ (M = Fe, Ni, Co, Mn) have been of interest for Li ion intercalation (5). Recently, lithium insertion in quaternary thiospinels like $(Cu_{3.31}Ge\square_{3.69})_{8a}[Fe_4Sn_{12}]_{16d}S_{32}$ has been reported (6). It is believed that the vacancies in the tetrahedral 8*a* sites result from a topotactic substitution of four Cu^{I} by one Ge^{IV}.

We have been interested in the synthesis and structural characterization of pure and doped thiospinels and in understanding the presence of vacancies in the Cu sites and in the Sn sites, if any, in these thiospinels. It may be noted that until now only one single-crystal study has been reported for quaternary thiospinels (7). We have studied recently in our laboratory new cation-deficient quaternary thiospinels like $Cu_{7.07}Ni_4Sn_{12}S_{32}$, $Cu_{7.38}Mn_4Sn_{12}S_{32}$, and $Cu_{5.47}Fe_{2.9}Sn_{13.1}S_{32}$. All of the above have been studied by single-crystal studies (unpublished work) and these show vacancies at the 8*a* site. As part of our ongoing studies on quaternary thiospinels, we have investigated the possibility of generating additional vacancies at the 8*a* site by doping higher-valent ions. We report here a single-crystal study of a Si-doped quaternary thiospinel, $Cu_{5.5}Si\square_{1.5}Fe_4Sn_{12}S_{32}$. We also report ^{119}Sn Mössbauer and ^{57}Fe Mössbauer studies of the above compound. Our studies are intended to investigate the presence of Cu site vacancies in higher-valent substituted thiospinels which would be useful in understanding the mechanism of Li ion conduction in these thiospinels. In addition, we have carried out resistivity studies of the Si-doped thiospinel at low temperatures (100–300 K).

EXPERIMENTAL

All manipulations were performed under a vacuum. Stoichiometric amounts of Cu (Acros Organics, Belgium, 99.9%), Fe (CDH, India, 99.5%), Sn (Acros Organics, Belgium, 99.9%), Si (Acros Organics, Belgium, 99 + %), and

[1]To whom correspondence should be addressed. Fax: 91-11-6854715. E-mail: ashok@chemistry.iitd.ernet.in.

0022-4596/01 $35.00

S (CDH, India, 98%) were loaded in the composition $Cu_{3.31}SiFe_4Sn_{12}S_{32}$ in a N_2-filled glove box. This was sealed in silica ampoules under high vacuum (10^{-5} Torr) and heated at 250°C for 2 days followed by annealing at 700°C for 6 days and then quenched at 680°C. After the reaction we observed the major phase to be present in the form of black cuboidal crystals, while a few brown crystals were also isolated. A powder X-ray diffraction pattern of the black cuboidal crystals (well ground) was recorded on a Phillips APD X- ray diffractometer with Cu$K\alpha$ radiation. It showed a pure cubic phase corresponding to the spinel structure. For the single-crystal structural study, the black crystals were selected, mounted in glass capillaries, and checked for singularity on a CAD-4 single-crystal diffractometer using Mo$K\alpha$ radiation. Though the crystals were initially sealed in glass capillaries, it was later found that the crystals are stable in air and undergo no change over a long period (at least for 6 months as observed in samples in our laboratory).

The Mössbauer spectra were recorded in transmission geometry using a constant acceleration-type Mössbauer spectrometer with a 10-mCi ^{57}Co source in a Rh matrix and 5-mCi ^{119m}Sn in a $BaSnO_3$ matrix for ^{57}Fe and ^{119}Sn spectra, respectively. A Xe-filled proportional counter was used as the detector. The data were acquired in the MCS mode in a multichannel analyzer containing 1024 channels. The velocity scale was calibrated using a ^{57}Co source and a metallic iron foil absorber. Mössbauer spectra of all the samples were recorded at 298 K. The spectra were fitted by a least-squares fitting program with Lorentzian profiles (8). All the isomer shift values were calculated with respect to the center of the α-Fe and $BaSnO_3$ spectrum.

Chemical analysis was performed to have an independent estimate of the amount of copper and silicon in the sample. The sample was dissolved in HCl and HNO_3 (long time digestion). Copper was estimated by atomic absorption spectroscopy using an ECIL AAS 4129 atomic absorption spectrometer. For estimation of silicon we have followed the procedure given elsewhere (9).

Four-probe resistivity measurements were carried out on compacted disks using silver contacts. The four probes (the outer two for current and the inner two for voltage) were aligned in a linear fashion with equal distance between each probe. Since the probe spacing and the thickness of the disk are comparable ($\sim$2 mm), the resistivity was calculated on the basis of the following equation,

$$\rho = (\pi t/\ln 2)\,(V/I),$$

where ρ stands for the resistivity, t is the thickness of the disk, V is the voltage drop measured, and I is the current passed through the sample. This takes care of the geometric factors while calculating resistivity. Temperature variation studies were carried out in a liquid nitrogen cryostat connected to a Lakeshore (321) temperature controller. A constant current source (Keithley 220) was used to provide the current through the sample and a microvoltmeter (Hewlett-Packard 34401A) was used to measure the voltage drop across the sample.

RESULTS AND DISCUSSION

The black cuboidal crystals obtained from the reaction (Experimental section) belong to the spinel structure as observed by powder X-ray diffraction studies. For further structural studies a crystal of size $0.10 \times 0.04 \times 0.04$ mm was selected for single-crystal X-ray crystallographic studies. A total of 409 reflections were collected in the θ range 3.42 to 29.97° ($0 \le h \le 14$, $0 \le k \le 14$, $0 \le l4 \le 14$). The data were corrected for Lorentz and polarization effects and for absorption (using three Ψ scans). The structure was developed by direct methods in the space group $Fd\bar{3}m$ and refined on F^2 (using SHELXTL 5.0). All the anisotropic thermal parameters were refined, as were the occupancies. A summary of the selected crystallographic data is listed in Table 1. Table 2 shows the refined atomic positions, occupancies, and isotropic thermal parameters for the crystal studied.

$Cu_{5.5}Si\square_{1.5}Fe_4Sn_{12}S_{32}$ crystallizes in the cubic $Fd\bar{3}m$ space group ($Z = 1$) with $a = 10.3322(6)$ Å (see Table 1). It is to be noted that the pure Fe compound, $Cu_2FeSn_3S_8$, has been found to crystallize in the $I4_1/a$ tetragonal space group with $a = 7.29$, $c = 10.31$ Å and $Z = 2$ (7). The Si-doped

TABLE 1
Selected Crystallographic Data for $Cu_{5.52(8)}Si_{1.04(8)}\square_{1.44}Fe_4Sn_{12}S_{32}$

Empirical formula	$Cu_{5.5}Si\square_{1.5}Fe_4Sn_{12}S_{32}$
Formula weight	3093.43
Temperature	293 (2) K
Wavelength	0.71073
Crystal color, habit	Black, cuboidal
Crystal size (mm)	$0.10 \times 0.04 \times 0.04$
Crystal system	Cubic
Space group	$Fd\bar{3}m$
a (Å)	10.3322(6)
Volume (Å^3), Z	1103.01(6), 1
$F(000)$	1389
Reflections collected	409
Theta range for data collection	3.42 to 29.97°
Data/restraints/parameters	101/0/10
GOF (on F^2)	1.115
$R_1{}^a$ [$I > 2\sigma(I)$]	0.0206
w$R_2{}^a$	0.0443
Extinction coefficient	0.0040(3)

$^aR_1 = \sum(|F_o - F_c|)/\sum(|F_o|)$. w$R_2 = [\sum w(F_o^2 - F_c^2)/\sum wF_o^4]^{1/2}$. GOF = $[\sum w(F_o^2 - F_c^2)/(n-p)]^{1/2}$, where n is the number of reflections and p is the number of parameters refined.

TABLE 2
Atomic Positions, Occupancies, and Thermal Parameters of $Cu_{5.5}Si\square_{1.5}Fe_4Sn_{12}S_{32}$

Atom	*x*	*y*	*z*	Occupancy	*U*(eq)
Cu	0.1250	0.1250	0.1250	0.69(1)	0.0177(4)
Si	0.1250	0.1250	0.1250	0.13(1)	0.0177(4)
Fe	0.5000	0.5000	0.5000	0.25	0.0118(3)
Sn	0.5000	0.5000	0.5000	0.75	0.0118(3)
S	0.74540(7)	0.74540(7)	0.74540(7)	1.00	0.0131(3)

compound (present study) shows vacancies in the 8*a* site (Table 2). All other occupancies were also refined. However, these sites led to full occupancies. (The refined occupancies of copper and silicon are within 3% of the values obtained by chemical analysis.)

The Si-doped Fe compound, $Cu_{5.5}Si\square_{1.5}Fe_4Sn_{12}S_{32}$ (present study), shows a very small decrease in Cu–S bond length from 2.320 Å in the parent compound, $Cu_8Fe_4Sn_{12}S_{32}$, to 2.319 Å in the doped compound studied here. This may be because of the doping of Si atoms as Si^{4+} is smaller in comparison to the size of Cu^+, which will lead to the smaller Cu–S bond length (10). The Fe/Sn–S distances do not show much change, being 2.536 Å in the former and 2.5365 Å in the Si-doped sample (Table 3).

In general, the substitution of four Cu atoms in $Cu_8Fe_4Sn_{12}S_{32}$ by one Si atom would lead to the formula $Cu_4SiFe_4Sn_{12}S_{32}$. Under these conditions, the oxidation states of Fe(II) and Sn(IV) atoms and the electroneutrality of the solid can be maintained. The results of our single-crystal X-ray diffraction studies, however, show an excess of Cu atoms in the 8*a* site, resulting in the formula $Cu_{5.5}Si\square_{1.5}Fe_4Sn_{12}S_{32}$. This in turn can take place only if the formal oxidation states of some cations decrease. ^{119}Sn and ^{57}Fe Mössbauer studies have been carried out on the title compound, to investigate the nature of Sn and Fe species in this compound. ^{119}Sn Mössbauer studies show the presence of both Sn^{II} and Sn^{IV} (Fig. 1). Approximately 86.4% of Sn is present in the IV oxidation state and 13.6% of Sn is present in the II oxidation state (Table 4). There have been some theoretical investigations (11) to understand Mössbauer results on an In-based thiospinel where the presence of Sn^{II} and Sn^{IV} are observed without any Sn^{III}.

TABLE 3
Bond Distances in Pure $Cu_2FeSn_3S_8$ (Ref. 7) and Si-Doped $Cu_{5.5}Si\square_{1.5}Fe_4Sn_{12}S_{32}$

Compound	Cu–4S (Å)	Si–4S (Å)	Fe/Sn–6S (Å)
$Cu_2FeSn_3S_8$	2.320(1)		2.536(1)
$Cu_{5.5}Si\square_{1.5}Fe_4Sn_{12}S_{32}$	2.3192(12)	2.3192(12)	2.5365(7)

The isomer shift values and quadrupole splitting values are in accordance with those given in the literature (5). We find a decrease in the isomer shift compared to that of the pure $Cu_8Fe_4Sn_{12}S_{32}$. The increase in the linewidth in the ^{119}Sn spectra of $Cu_{5.5}Si\square_{1.5}Fe_4Sn_{12}S_{32}$ as compared with those of $Cu_8Fe_4Sn_{12}S_{32}$ is similar in sign and slightly larger than that found in $Cu_8Fe_4Sn_{12}S_{32}$ (Fig. 1). Similar behavior has also been observed for the Ge-doped thiospinel, $Cu_{3.31}Ge Fe_4Sn_{12}S_{32}$ (6), where vacancies in the Cu site due to Ge substitution have been observed. The Mössbauer data are compared in Table 4. In both of the above cation-deficient solids, the enhanced broadening is in good agreement with the presence of slightly different Sn^{IV} environments. In $Cu_8Fe_4Sn_{12}S_{32}$, all the tetrahedral neighbors are Cu atoms, while three different neighbors, Cu, Si, and vacancies, are present in our compound $Cu_{5.5}Si\square_{1.5}Fe_4Sn_{12}S_{32}$. The presence of these three neighbors decreases the symmetry around the Sn^{IV} cations, leading to an increase in the linewidth of the peak.

We recorded the ^{57}Fe Mössbauer spectrum of the above compound. A decrease in the isomer shift and quadrupole

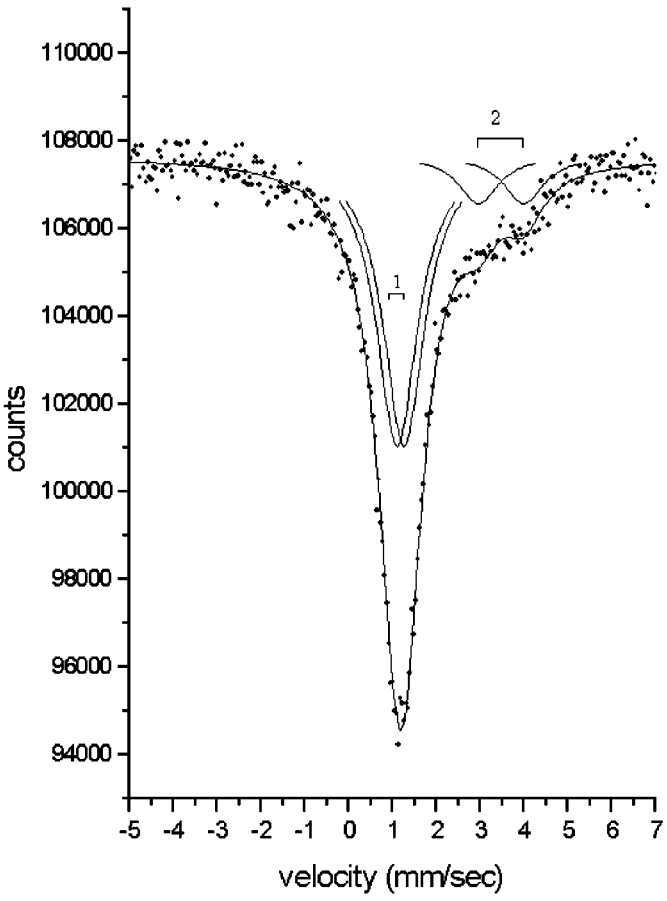

FIG. 1. ^{119}Sn Mössbauer spectrum of $Cu_{5.5}Si\square_{1.5}Fe_4Sn_{12}S_{32}$ at 298 K. Peaks labelled "1"correspond to Sn^{IV}, and peaks labelled "2" correspond to Sn^{II}.

TABLE 4
Hyperfine Parameters of ^{119}Sn Mössbauer Spectra of $Cu_2FeSn_3S_8$, $Li_xCu_{3.31}GeFe_4Sn_{12}S_{32}$ ($x = 12$), and $Cu_{5.5}Si\square_{1.5}Fe_4Sn_{12}S_{32}$: Isomer Shift ($\delta$), Quadrupole Splitting (Δ), and Full-Width at Half-Maximum (T)

Compound	δ/mm s^{-1}	Δ/mm s^{-1}	T/mm s^{-1}	Attribution	Ref.
$Cu_8Fe_4Sn_{12}S_{32}$	1.246(1)	0.321(6)	0.863(6)	Sn^{IV}	6
$Li_xCu_{3.31}GeFe_4Sn_{12}S_{32}$	1.196(6)	0.41(1)	0.86(2)	Sn^{IV} (89%)	6
	3.25(5)	0.55(8)	0.9(1)	Sn^{II} (11%)	
$Cu_{5.5}Si\square_{1.5}Fe_4Sn_{12}S_{32}$	1.18(3)	0.16(3)	1.13(3)	Sn^{IV} (86.4%)[a]	Present study
	3.46(3)	1.03(3)	1.09(3)	Sn^{II} (13.6%)[b]	Present study

[a]Corresponds to peaks labelled "1" in Fig. 1.
[b]Corresponds to peaks labelled "2" in Fig. 1.

splitting has been observed in $Cu_{5.5}Si\square_{1.5}Fe_4Sn_{12}S_{32}$ in the same way as in the copper-deficient compound $Cu_{8-x}Fe_4Sn_{12}S_{32}$ (5) compared to that of $Cu_8Fe_4Sn_{12}S_{32}$ (composed of two peaks centered at 0.2 and 1.3 mm s^{-1}). The decrease of the isomer shift and quadrupole splitting after Cu extraction in $Cu_{8-x}Fe_4Sn_{12}S_{32}$ is normally attributed to a slight reduction of the screening effect (fewer electrons) caused by the partial oxidation of Fe^{II} to Fe^{III}. This correlates well with the stoichiometry and the presence of Sn(II) and Sn(IV) in the compound. Similar behavior has been observed in the Ge-doped compound $Cu_{3.31}Ge\square_{3.69}Fe_4Sn_{12}S_{32}$ (6). Thus, by comparison of the two cation-deficient compounds, we can conclude that the copper defect in $Cu_{5.5}Si\square_{1.5}Fe_4Sn_{12}S_{32}$ induces part of Fe^{II} to Fe^{III} (Fig. 2). However, we could not resolve the separate contributions of Fe^{II} and Fe^{III} to the profile (this is also found in the Ge-doped thiospinel (6)) and is probably due to the electron transfer between Fe^{II} and Fe^{III}, which does not allow the two species to be distinguished by Mössbauer spectroscopy.

We have measured the electrical resistivity of the Si-doped quaternary thiospinels, $Cu_{5.5}Si\square_{1.5}Fe_4Sn_{12}S_{32}$, in the temperature range 100 K to 300 K. We find that it behaves like a semiconductor from room temperature down to 100 K. From the log ρ vs $1/T$ Arrhenius plots (see inset of Fig. 3) the band gap is found to be 0.107 eV in the temperature range 170 K to 300 K. The room temperature resistivity is around 1×10^2 Ω-cm (Fig. 3.).

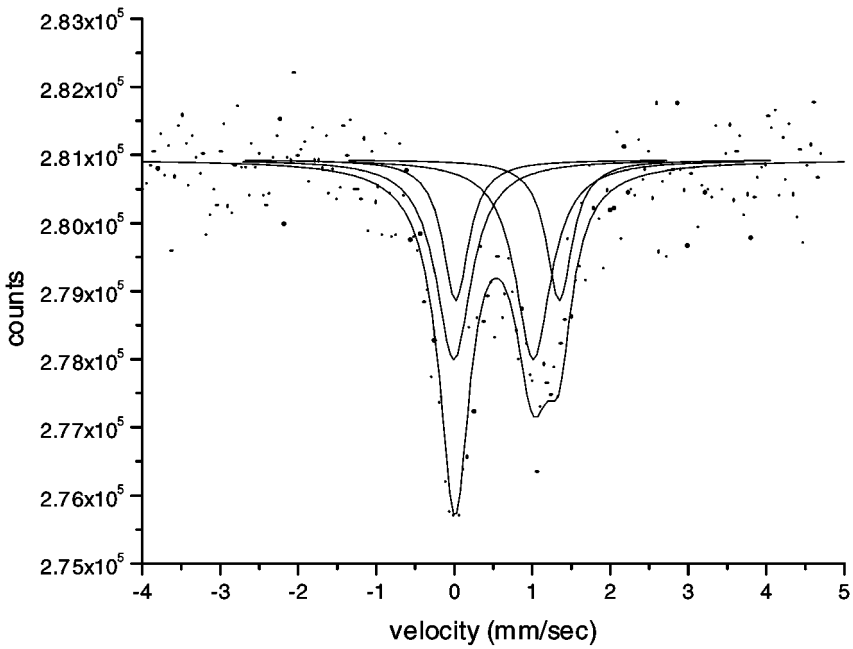

FIG. 2. ^{57}Fe Mössbauer spectrum of $Cu_{5.5}Si\square_{1.5}Fe_4Sn_{12}S_{32}$ at 298 K.

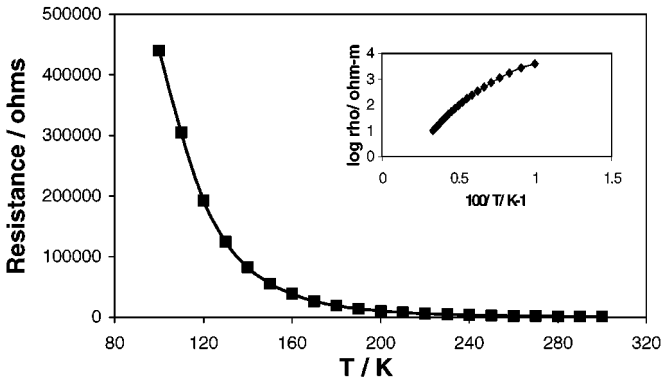

FIG. 3. Variation of the electrical resistance of $Cu_{5.5}Si\square_{1.5}Fe_4Sn_{12}S_{32}$ with temperature. The inset shows the plot of the logarithm of resistivity vs $100/T$.

CONCLUSIONS

A new Si-doped cation-deficient quaternary thiospinel, $Cu_{5.5}Si\square_{1.5}Fe_4Sn_{12}S_{32}$, has been structurally characterized. Additional vacancies in the copper site are compensated by the higher valence of the Si^{IV} ion and the presence of Sn^{II}/Sn^{IV} as well as of Fe^{II}/Fe^{III} species. The above thiospinel was found to be a semiconductor with a low band gap. The availability of a sufficient number of vacancies in the 8*a* site in this compound makes it ideal for future lithiation studies. Subsequent structural analysis of the lithiated products is planned for execution along with electrochemical studies.

ACKNOWLEDGEMENTS

We thank Dr. S. Ghosh of School of Physical Sciences, JNU, New Delhi, for access to the electrical resistivity facility. A. K. G. thanks the Department of Science and Technology, Government of India, for financial assistance.

REFERENCES

1. W. R. McKinnon and J. R. Dahn, *Solid State Commun.* **52,** 254 (1984).
2. E. Gocke, R. Schöllhorn, G. Aselmann, and E. Muller-Warmuth, *Inorg. Chem.* **26,**1805 (1987).
3. A. C. W. P. James, B. Ellis, and J. B. Goodenough, *Solid State Ionics* **27,** 45 (1988); **24,** 143 (1989).
4. M. Eisenberg, *J. Electrochem. Soc.* **127,** 2382 (1980).
5. P. Lavela, J. L. Tirado, J. Morales, J. Olivier-Fourcade, and J. C. Jumas, *J. Mater. Chem.* **6,** 41 (1996).
6. C. Bousquet, C. Perez Vicente, A. Kramer, J. Olivier-Fourcade, and J. C. Jumas, *J. Mater. Chem.* **6,** 1399 (1998).
7. J. C. Jumas, E. Philippot, and M. Maurin, *Acta Crystallogr., Sect. B* **35,** 2195 (1979).
8. E. von Meerwal, *Comput. Phys. Commun.* **9,** 117 (1975).
9. G. H. Jeffery, J. Bassett, J. Medham, and R. C. Denny, *in* "Vogel's Textbook of Quantitative Chemical Analysis," 5th Ed., p. 703. ELBS, Great Britain, 1991.
10. R. D. Shannon, *Acta Crystallogr., Sect. A* **32,** 751 (1976).
11. J. P. Connerade, J. C. Jumas, and J. Olivier-Fourcade, *J. Solid State Chem.* **152,** 533 (2000).